View Article Online
View Journal

ChemComm

Chemical Communications

Accepted Manuscript

This article can be cited before page numbers have been issued, to do this please use: W. Qian, M. Zuo, G. Sun, Y. Chen, T. Han, X. Hu, R. Wang and L. Wang, *Chem. Commun.*, 2020, DOI: 10.1039/D0CC02962A.

ROYAL SOCIETY OF CHEMISTRY

rsc.li/chemcomm

View Article Online
DOI: 10.1039/D0CC02962A

COMMUNICATION

The Construction of AIE-Based Controllable Singlet Oxygen Generation System Directed by Supramolecular Strategy †

Received 00th January 20xx,
Accepted 00th January 20xx

DOI: 10.1039/x0xx00000x

Weirui Qian,[a] Minzan Zuo,[a] Guangping Sun,[a] Yuan Chen,[a] Tingting Han,[a] Xiao-Yu Hu,*[b] Ruibing Wang,[c] and Leyong Wang*[a]

An aggregation-induced emission (AIE) based smart singlet oxygen ($^1O_2$) generation system has been successfully fabricated based on supramolecular host–guest assembly. The controllable $^1O_2$ generation can be achieved by conveniently changing the molar ratio between the macrocyclic host (WP5) and the guest molecule (TPEPY). Moreover, reversible control of $^1O_2$ generation and fluorescence emission of supramolecular nanoassemblies can be achieved via adding Fe^{3+} and EDTA, which allows qualitatively monitoring the singlet oxygen generation efficiency by naked eye.

Singlet oxygen ($^1O_2$) is a kind of reactive oxygen species (ROS), which can be generated by photosensitization between photosensitizer (PS) and molecular oxygen ($^3O_2$) upon irradiation.[1] Due to the broad application of $^1O_2$ in sewage treatment, photodynamic therapy (PDT), and photochemical synthesis,[2] PS which can generate $^1O_2$ is of great interest. While great progress has been achieved to PS with high efficiency, more recently the design of a smart system in which $^1O_2$ generation is tunable has attracted growing attentions among researchers. For example, Guo et al. proposed a concept of biomarker displacement activation, which could realize the reversible control of $^1O_2$ generation.[3] Due to the controllability of $^1O_2$ generation, these smart systems have potential applications in the fields of PDT (showing better therapeutic efficiency) and controlled photocatalysis.[4]

However, most of the reported systems focus on traditional PSs, which suffer from weak fluorescence intensity as well as inefficient $^1O_2$ production in aggregation state due to the aggregation-caused quenching (ACQ) phenomenon.[5] Since hydrophobic organic PSs prefer to aggregate in water, such ACQ characteristics greatly limit their applications.[6] Hence, designing smart $^1O_2$ generation system in aqueous phase that can avoid such shortcomings remains a challenging task. Fortunately, the above issues can be solved by developing a class of PSs featuring aggregation-induced emission (AIE) characteristics. The $^1O_2$ quantum yield for most of them are higher than Photofrin (0.28), a kind of clinically used PS.[7] Moreover, it has been confirmed that AIE-based PSs are able to offer sufficient $^1O_2$ production in aggregation state owing to the prohibition of nonradiative transition.[2b,7] However, the fabrication of AIE-based controllable $^1O_2$ generation system in response to environmental changes was rarely reported, perhaps due to complicated synthesis steps by covalently introducing functional groups.[8] Considering that supramolecular strategy can endow a system with controllable stimuli-responsiveness and avoid multiple synthesis steps through noncovalent molecular recognition,[9] the design of AIE-based controllable $^1O_2$ generation system in aqueous phase directed by host–guest interaction is highly appealing.[10]

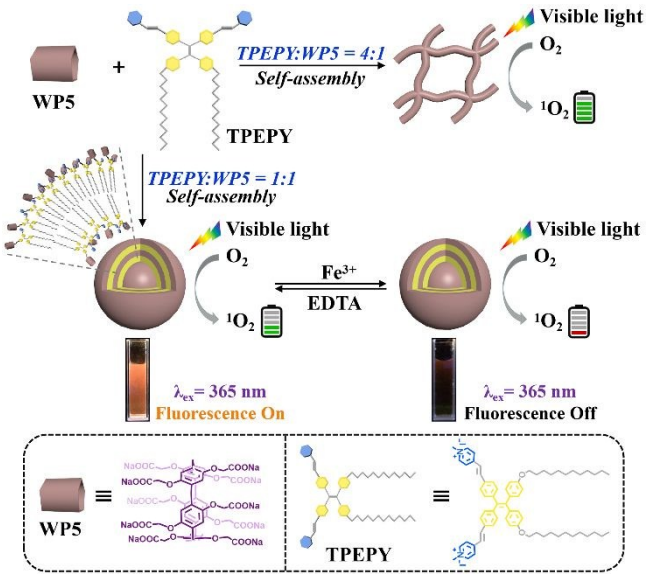

Scheme 1 Schematic illustration of the AIE-based smart singlet oxygen generation system directed by supramolecular strategy.

[a] Key Laboratory of Mesoscopic Chemistry of MOE, Jiangsu Key Laboratory of Advanced Organic Materials, School of Chemistry and Chemical Engineering, Nanjing University, Nanjing, 210023, China. E-mail: lywang@nju.edu.cn (LW).
[b] Applied Chemistry Department, School of Material Science and Engineering, Nanjing University of Aeronautics and Astronautics, Nanjing, 211100, China. E-mail: huxy@nuaa.edu.cn (XH).
[c] State Key Laboratory of Quality Research in Chinese Medicine, Institute of Chinese Medical Sciences, University of Macau, Taipa, Macau, China.

† Electronic Supplementary Information (ESI) available: Experimental data and NMR spectra *etc*. See DOI: 10.1039/x0xx00000x

Herein, a novel AIE-based smart singlet oxygen generation system based on supramolecular host–guest assembly has been reported in aqueous phase (Scheme 1). The compact combination between the macrocyclic host and the guest molecule may greatly change the D–A (donor–acceptor push–pull) structure of the guest, resulting in the change of $^1O_2$ generation efficiency. Thus, the controllable $^1O_2$ generation could be achieved by conveniently changing the molar ratio between the host and the guest molecule. In addition, reversible control of $^1O_2$ generation and the corresponding fluorescence emission of supramolecular nanoassemblies could be achieved via adding Fe^{3+} and EDTA, allowing qualitatively monitoring the efficiency of $^1O_2$ generation by naked eye.

TPEPY was synthesized as guest molecule by using 4,4′-dibromobenzophenone and 4,4′-dihydroxybenzophenone as the starting material (Scheme S1 and Fig. S1–S9, ESI†). **TPEPY** is a typical AIE-based PS with excellent $^1O_2$ generation efficiency and photostability, which exhibits a suitable D–A structure with alkoxy chain modified tetraphenylethylene as the electron-donating moiety, and pyridinium as the electron-accepting moiety. It is widely reported that proper electron donating and accepting groups are of great importance since they determine the D–A structure of the designed AIE-based PS, which influences the $^1O_2$ generation efficiency.[7]

Considering that the electron rich cavity of macrocyclic molecule (host) can strongly bind with the electron-deficient pyridinium moiety due to electrostatic effect and hydrophobic interaction,[11] it is inferred that the D–A structure of guest molecule will be greatly changed upon its close combination with suitable host compound, resulting in the inhibition of $^1O_2$ generation. To verify the assumption above, various macrocyclic host molecules with similar cavity sizes,[12] including α-cyclodextrin (**α-CD**), cucurbituril[6] (**CB6**), 4-sulfocalix[4]arene (**CX4**), and water-soluble pillar[5]arene (**WP5**), were used to investigate the $^1O_2$ generation efficiency of the host–guest mixtures. Initially, the thermodynamics between the host and the guest were investigated prior to the $^1O_2$ generation efficiency. Due to the host–guest inclusion complex formed from macrocyclic molecule and **TPEPY** tended to self-aggregate in water, **G′** (1-methylpyridinium iodide) with the same electron-accepting moiety of **TPEPY** was taken as a model guest molecule. Isothermal titration calorimetry (ITC) experiments confirmed that the association constant between **TPEPY** and **α-CD** was negligible, while the association constant for the supramolecular complexes **TPEPY**-**CX4** and **TPEPY**-**WP5** was 1.2×10^4 and 2.2×10^4 M^{-1}, respectively (Fig. S10, ESI†). Because of the poor solubility of **CB6**, the association constant between **TPEPY** and **CB6** was negligible likewise.

Considering that **TPEPY** has a wide absorption range in visible light region and exhibits orange fluorescence with a strong emission band peaking at the wavelength of 596 nm (Fig. S11, ESI†), visible light was used to excite **TPEPY**. After irradiation with visible light for 300 s, nearly 70% of 9,10-anthracenediyl-bis(methylene)dimalonic acid (ABDA), a commercially available $^1O_2$ indicator, was consumed in the presence of free **TPEPY** in water at a decomposition rate of 27.2 μmol min^{-1}. As expected, when different macrocycles were added, the decomposition rates for the supramolecular complexes **TPEPY**-**α-CD**, **TPEPY**-**CB6**, **TPEPY**-**CX4**, and **TPEPY**-**WP5** were evaluated to be 25.6, 26.4, 11.2, and 8.8 μmol min^{-1}, respectively (Fig. 1a and Fig. S12, ESI†). The above results demonstrate that the $^1O_2$ generation efficiency of **TPEPY** can be significantly suppressed upon its binding with **CX4** or **WP5**, and **WP5** was more effective than **CX4**. However, due to the negligible binding capacity between **TPEPY** and **α-CD** or **CB6**, the corresponding D–A structure was not influenced, thus the $^1O_2$ generation efficiency remained unchanged.

Taking into account the predominate ability of **WP5** in inhibiting the production of $^1O_2$, the $^1O_2$ generation efficiency of **TPEPY** with varied concentrations of **WP5** was further evaluated (Fig. 1b and Fig. S13, ESI†). It turned out that the $^1O_2$ generation efficiency was gradually suppressed with an increasing amount of **WP5**, which decreased to 20% of its original value in the presence of 4 equiv. of **WP5**. Therefore, the controllable $^1O_2$ generation could be conveniently achieved by changing the molar ratio between the **WP5** host and **TPEPY** guest. To verify that the above phenomena were caused by host–guest interaction, not merely simple electrostatic interaction, hydroquinone-O,O′-diacetic acid disodium salt (**M**), the fragment unit of **WP5**, was taken as a control compound to evaluate the $^1O_2$ generation efficiency.

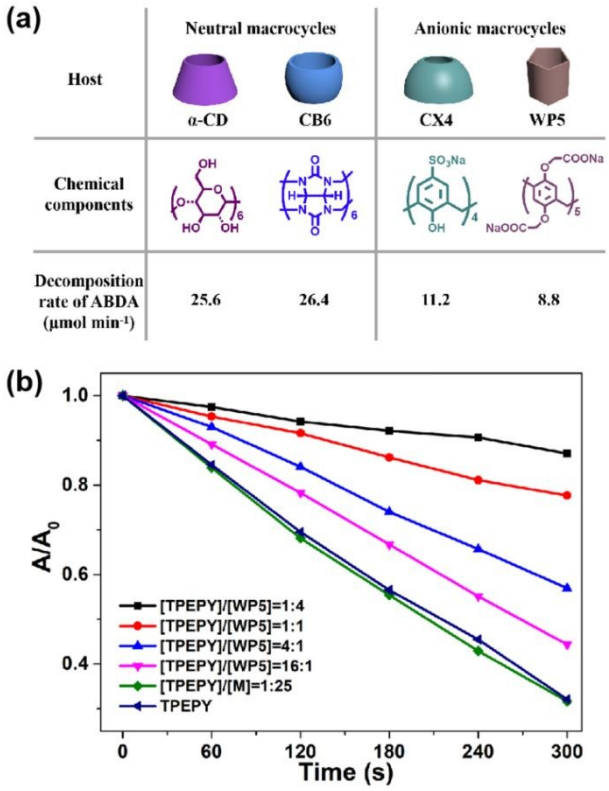

Fig. 1 (a) Decomposition rate of ABDA in the presence of **TPEPY** with different macrocyclic molecules upon visible light irradiation. (b) Normalized degradation percentages of ABDA at 401 nm in the presence of **TPEPY** with varied concentrations of **WP5** under visible light irradiation. **M** represents the fragment unit of **WP5**.

As presented in Fig. 1b, the $^1O_2$ generation efficiency of **TPEPY-M** mixture displayed almost no change compared with free **TPEPY**, which was consistent with our hypothesis. Moreover, **RB** (Rose Bengal), a commercial available PS, was also taken as a control compound to further investigate the $^1O_2$ generation efficiency affected by the change of D–A structure. Results revealed that **RB** showed limited changes in $^1O_2$ generation efficiency in the presence of **WP5** (Fig. S14, ESI†), indicating that **WP5** can function as an electron donor to specifically regulate the $^1O_2$ generation efficiency of AIE-based PSs with an electron-accepting moiety.

Interestingly, compared with free **TPEPY** solution, **TPEPY-WP5** solution showed notable opalescence as well as obvious Tyndall effect (Fig. S15, ESI†), suggesting the existence of abundant nanoaggregates. The above phenomenon mainly attributes to the further self-assembly of **WP5⊃TPEPY** supramolecular amphiphilic complex in water. Although AIE-based PSs are able to offer effective $^1O_2$ production in aggregated state, the dense packing of PSs in the nanocore can still result in compromised $^1O_2$ generation efficiency due to the limited exposure to oxygen.[13] Therefore, to understand the regulation mechanism of this smart $^1O_2$ generation system more clearly, the aggregation behavior of supramolecular amphiphilic complex is necessary to be investigated.

The best molar ratio between **WP5** and **TPEPY** for fabricating supramolecular nanoassemblies was determined to be 4:1 ([**TPEPY**]/[**WP5**]) by optical transmittance tests (Fig. S16, ESI†). Based on the obtained molar ratio, the critical aggregation concentration (CAC) of **WP5⊃TPEPY** nanoassemblies was confirmed to be 1.3×10^{-5} M (Fig. S17, ESI†). Subsequently, the morphology and size of the self-assembled nanoaggregates formed by **WP5⊃TPEPY** complex were determined by transmission electron microscopy (TEM) and dynamic light scattering (DLS) measurements, respectively. As shown in Fig. 2, upon decreasing the molar ratio ([**TPEPY**]/[**WP5**]) from 8:1 to 4:1 (the best molar ratio), the morphology of nanoassemblies changed from linked nanoparticles to nanonetworks which probably formed through the further fusion of the nanoparticles. However, when the molar ratio was further decreased to 1:1, the morphology of nanoassemblies changed back to nanoparticles with smaller size and uniform distribution. Subsequently, DLS results revealed that nanoparticles formed at the molar ratio of 1:1 ([**TPEPY**]/[**WP5**]) displayed a narrow size distribution with an average diameter of 198 nm, whereas, the nanoassemblies obtained at the molar ratio of 4:1 and 8:1 ([**TPEPY**]/[**WP5**]) were both in the microscale level, which correlated well with the TEM results. The above phenomena are mainly caused by the changeable amounts of nanoassemblies at different molar ratio. Moreover, the stability of above three kinds of nanoassemblies was investigated by detecting their dimensional changes based on DLS experiments (Fig. S18, ESI†), and the results showed that these supramolecular nanoaggregates were stable after incubating for 2 days. Although the best molar ratio for constructing nanoassemblies was 4:1 ([**TPEPY**]/[**WP5**]), the best molar ratio for the inhibition of $^1O_2$ generation was 1:4

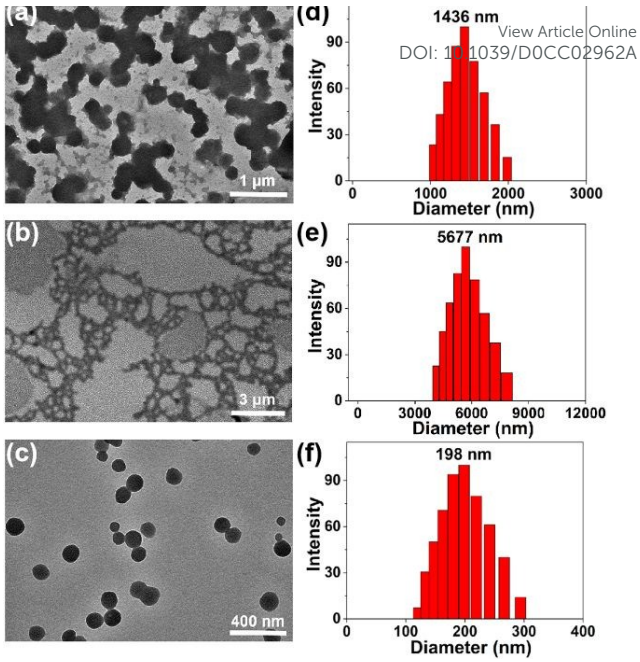

Fig. 2 TEM images of **WP5⊃TPEPY** nanoassemblies: (a) [**TPEPY**]/[**WP5**] = 8:1, (b) [**TPEPY**]/[**WP5**] = 4:1, and (c) [**TPEPY**]/[**WP5**] = 1:1. DLS data of **WP5⊃TPEPY** nanoassemblies: (d) [**TPEPY**]/[**WP5**] = 8:1, (e) [**TPEPY**]/[**WP5**] = 4:1, and (f) [**TPEPY**]/[**WP5**] = 1:1.

([**TPEPY**]/[**WP5**]). Therefore, combining the analyses of $^1O_2$ generation efficiency at different molar ratios and the aggregation behavior of **WP5⊃TPEPY** complex, it can be concluded that the main regulation mechanism for this smart $^1O_2$ generation system should attribute to the change of D–A structure of the **TPEPY** guest upon its strong combination with **WP5** based on host–guest interaction.

Moreover, **WP5⊃TPEPY** supramolecular nanoassemblies could further realize reversible control of $^1O_2$ generation and fluorescence emission via alternating addition of Fe^{3+} and EDTA. As seen in Fig. 3a, the $^1O_2$ generation efficiency was drastically suppressed when Fe^{3+} was added to the **WP5⊃TPEPY** solution ([**TPEPY**]/[**WP5**] = 1:1) (For details, see Fig. S19, ESI†). Meanwhile, the fluorescence was obviously quenched in 10 minutes (Fig. 3c). However, no obvious changes of $^1O_2$ generation efficiency could be observed for the **RB** group after the addition of Fe^{3+}, revealing the specific selectivity of this system to Fe^{3+} (Fig. S20, ESI†). The above phenomena were mainly caused by the complexation between **WP5** and Fe^{3+}, resulting in the efficient photo-induced electron transfer (PET) from **TPEPY** to the formed **WP5**-Fe^{3+} complex.[3,14] With respect to the free **TPEPY** solution, after the addition of Fe^{3+}, the $^1O_2$ generation was inhibited but fluorescence remained unchanged (Fig. 3b, 3d). This was probably related with the diminished PET efficiency of free **TPEPY** compared with the **WP5⊃TPEPY** complex, due to the existed charge repulsion between **TPEPY** and Fe^{3+}. Moreover, considering that the counter ion I^- is closely related to the $^1O_2$ generation efficiency of AIE-based PSs,[7a] we suspected that the chemical equilibrium between Fe^{3+} and I^- may also play a synergistic

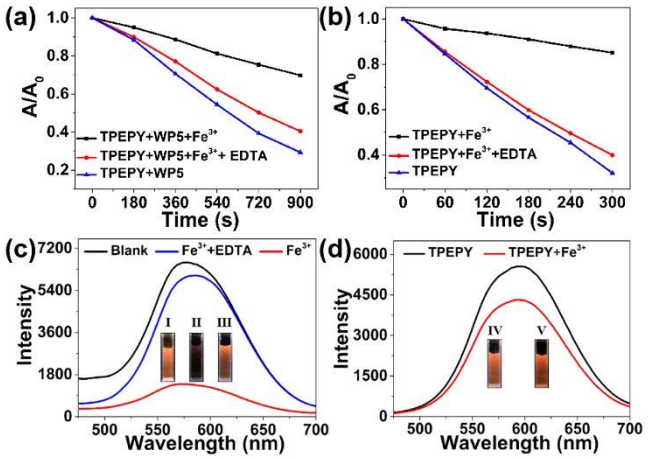

Fig. 3 Normalized degradation percentages of ABDA at 401 nm in the presence of **WP5⊃TPEPY** nanoassemblies (a), and **TPEPY** (b) upon adding Fe^{3+} and EDTA under visible light irradiation. Fluorescence emission spectra of **WP5⊃TPEPY** nanoassemblies (c), and **TPEPY** (d) upon adding Fe^{3+} and EDTA. Inset: Fluorescent images of **WP5⊃TPEPY** (Ⅰ), **WP5⊃TPEPY**+Fe^{3+} (Ⅱ), **WP5⊃TPEPY**+Fe^{3+}+EDTA (Ⅲ), **TPEPY** (Ⅳ), and **TPEPY**+Fe^{3+} (Ⅴ) (λ_{ex} = 365 nm). [**TPEPY**] = 15 μM, [**WP5**] = 15 μM, [Fe^{3+}] = 0.18 mM, and [EDTA] = 4.50 mM.

role in the inhibition of $^1O_2$ generation.[15]

Subsequently, when EDTA, a strong chelator of Fe^{3+}, was added to the free **TPEPY** or **WP5⊃TPEPY** solution pre-treated with Fe^{3+}, the $^1O_2$ generation efficiency could be reversibly recovered (Fig. 3a, 3b). What's more, for the **WP5⊃TPEPY** nanoassemblies, the fluorescence intensity could also be recovered, reaching to 90% of its original values (Fig. 3c). Therefore, the reversible control of $^1O_2$ generation and fluorescence emission of **WP5⊃TPEPY** supramolecular nanoassemblies could be achieved via adding Fe^{3+} and EDTA, making it possible to qualitatively monitor the $^1O_2$ generation efficiency by naked eye rather than using indicator.

In summary, a novel AIE-based smart singlet oxygen generation system based on supramolecular strategy has been successfully developed in aqueous phase, where the $^1O_2$ generation is tunable. The strong host–guest combination between **WP5** and **TPEPY** may greatly change the D–A structure of the guest, and thus controllable $^1O_2$ generation could be achieved by conveniently changing the molar ratio between the host and the guest molecule. Moreover, reversible control of $^1O_2$ generation and fluorescence emission of supramolecular nanoassemblies could be achieved through adding Fe^{3+} and EDTA, making it possible to qualitatively monitor the $^1O_2$ generation efficiency by naked eye. The present work provides a new strategy for the construction of tunable $^1O_2$ generation system based on simple supramolecular strategy, which might have potential applications in the fields of controlled photocatalysis and regulated photodynamic therapy.

This work was supported by the National Natural Science Foundation of China (No. 21572101, 21871136), and the Natural Science Foundation of Jiangsu Province (No. BK20180055). L. Wang is grateful to UM Macao Distinguished Visiting Scholar Scheme. We thank the referees for their fruitful suggestions to improve the quality of this manuscript.

Conflicts of interest

There are no conflicts to declare.

Notes and references

1 a) C. Zhang, Y. Zhao, D. Li, J. Liu, H. Han, D. He, X. Tian, S. Li, J. Wu and Y. Tian, *Chem. Commun.*, 2019, **55**, 1450–1453; b) V. Kabanov, D. J. Press, R. P. S. Huynh, G. K. H. Shimizu and B. Heyne, *Chem. Commun.*, 2018, **54**, 6320–6323.
2 a) K. Yang, J. Wen, S. Chao, J. Liu, K. Yang, Y. Pei and Z. Pei, *Chem. Commun.*, 2018, **54**, 5911–5914; b) W. Wu, D. Mao, S. Xu, F. Hu, X. Li, D. Kong and B. Liu, *Chem*, 2018, **4**, 1937–1951; c) J. Han, K. Liu, R. Chang, L. Zhao and X. Yan, *Angew. Chem., Int. Ed.*, 2019, **58**, 2000–2004.
3 J. Gao, J. Li, W.-C. Geng, F.-Y. Chen, X. Duan, Z. Zheng, D. Ding and D.-S. Guo, *J. Am. Chem. Soc.*, 2018, **140**, 4945–4953.
4 a) K. Hirakawa, M. Harada, S. Okazaki and Y. Nosaka, *Chem. Commun.*, 2012, **48**, 4770–4772; b) G. Liu, X. Xu, Y. Chen, X. Wu, H. Wu and Y. Liu, *Chem. Commun.*, 2016, **52**, 7966–7969; c) I. Roy, S. Bobbala, R. M. Young, Y. Beldjoudi, M. T. Nguyen, M. M. Cetin, J. A. Cooper, S. Allen, O. Anamimoghadam, E. A. Scott, M. R. Wasielewski and J. F. Stoddart, *J. Am. Chem. Soc.*, 2019, **141**, 12296–12304; d) W. Hu, T. He, H. Zhao, H. Tao, R. Chen, L. Jin, J. Li, Q. Fan, W. Huang, A. Baev and P. N. Prasad, *Angew. Chem., Int. Ed.*, 2019, **131**, 11222–11228.
5 D. Wang, M. M. S. Lee, G. Shan, R. T. K. Kwok, J. W. Y. Lam, H. Su, Y. Cai and B.-Z. Tang, *Adv. Mater.*, 2018, **30**, 1802105.
6 D. Wang, H. Su, R. T. K. Kwok, X. Hu, H. Zou, Q. Luo, M. M. S. Lee, W. Xu, J. W. Y. Lam and B.-Z. Tang, *Chem. Sci.*, 2018, **9**, 3685–3693.
7 a) F. Hu, S. Xu and B. Liu, *Adv. Mater.*, 2018, **30**, 1801350; b) Y. Zheng, H. Lu, Z. Jiang, Y. Guan, J. Zou, X. Wang, R. Cheng and H. Gao, *J. Mater. Chem. B*, 2017, **5**, 6277–6281.
8 Y. Yuan, S. Xu, C.-J. Zhang, R. Zhang and B. Liu, *J. Mater. Chem. B*, 2016, **4**, 169–176.
9 a) S.-B. Yu, Q. Qi, B. Yang, H. Wang, D.-W. Zhang, Y. Liu and Z.-T. Li, *Small*, 2018, **14**, 1801037; b) B. Tang, W.-L. Li, Y. Chang, B. Yuan, Y. Wu, M.-T. Zhang, J.-F. Xu and X. Zhang, *Angew. Chem., Int. Ed.*, 2019, **131**, 15672–15677; c) X.-H. Wang, N. Song, W. Hou, C.-Y. Wang, Y. Wang, J. Tang and Y.-W. Yang, *Adv. Mater.*, 2019, **31**, 1903962; d) W. Chen, C. Guo, Q. He, X. Chi, V. M. Lynch, Z. Zhang, J. Su, H. Tian and J. L. Sessler, *J. Am. Chem. Soc.*, 2019, **141**, 14798–14806.
10 a) C. Chen, X. Ni, H.-W. Tian, Q. Liu, D.-S. Guo and D. Ding, *Angew. Chem., Int. Ed.*, 2020, DOI: 10.1002/anie.201916430; b) L. Shao, Y. Pan, B. Hua, S. Xu, G. Yu, M. Wang, B. Liu and F. Huang, *Angew. Chem., Int. Ed.*, 2020, DOI: 10.1002/ange.202000338.
11 a) X.-Y. Hu, X. Liu, W. Zhang, S. Qin, C. Yao, Y. Li, D. Cao, L. Peng and L. Wang, *Chem. Mater.*, 2016, **28**, 3778–3788.
12 a) H. Bakirci, A. L. Koner and W. M. Nau, *J. Org. Chem.*, 2005, **70**, 9960–9966; b) K. Kim, N. Selvapalam, Y. H. Ko, K. M. Park, D. Kim and J. Kim, *Chem. Soc. Rev.*, 2007, **36**, 267–279; c) Y. Chen, Y.-M. Zhang and Y. Liu, *Chem. Commun.*, 2010, **46**, 5622–5633; d) M. Xue, Y. Yang, X. Chi, Z. Zhang and F. Huang, *Acc. Chem. Res.*, 2012, **45**, 1294–1308.
13 Y. Li, Q. Wu, M. Kang, N. Song, D. Wang and B.-Z. Tang, *Biomaterials*, 2020, **232**, 119749.
14 a) M. Zuo, W. Qian, T. Li, X.-Y. Hu, J. Jiang and L. Wang, *ACS Appl. Mater. Interfaces*, 2018, **10**, 39214–39221; b) P. Wei, D. Li, B. Shi, Q. Wang and F. Huang, *Chem. Commun.*, 2015, **51**, 15169–15172.
15 P. A. Nikolaychuk and A. O. Kuvaeva, *J. Chem. Educ.*, 2016, **93**, 1267–1269.

View Article Online
DOI: 10.1039/D0CC02962A

Graphical Abstract

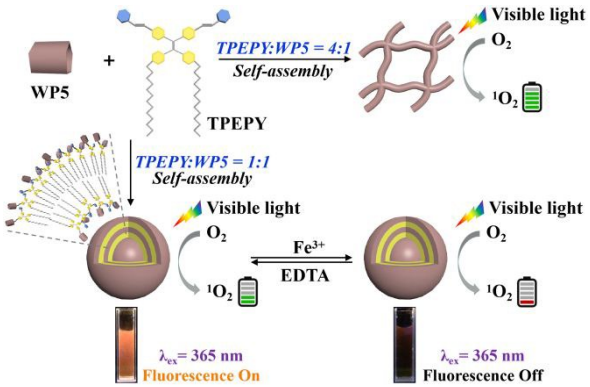

An aggregation-induced emission based controllable singlet oxygen generation system has been successfully fabricated in aqueous phase based on supramolecular host–guest assembly.